J|A|C|S ARTICLES

Published on Web 03/23/2009

DFT and ONIOM(DFT:MM) Studies on Co−C Bond Cleavage and Hydrogen Transfer in B_{12}-Dependent Methylmalonyl-CoA Mutase. Stepwise or Concerted Mechanism?

Xin Li,[†] Lung Wa Chung,[†] Piotr Paneth,[‡] and Keiji Morokuma*,[†]

Fukui Institute for Fundamental Chemistry, Kyoto University, Kyoto 606-8103, Japan, and Institute of Applied Radiation Chemistry, Technical University of Lodz, Zeromskiego 116, 90-924 Lodz, Poland

Received September 28, 2008; E-mail: morokuma@fukui.kyoto-u.ac.jp

Abstract: The considerable protein effect on the homolytic Co−C bond cleavage to form the 5′-deoxyadenosyl (Ado) radical and cob(II)alamin and the subsequent hydrogen transfer from the methylmalonyl-CoA substrate to the Ado radical in the methylmalonyl-CoA mutase (MMCM) have been extensively studied by DFT and ONIOM(DFT/MM) methods. Several quantum models have been used to systematically study the protein effect. The calculations have shown that the Co−C bond dissociation energy is very much reduced in the protein, compared to that in the gas phase. The large protein effect can be decomposed into the cage effect, the effect of coenzyme geometrical distortion, and the protein MM effect. The largest contributor is the MM effect, which mainly consists of the interaction of the QM part of the coenzyme with the MM part of the coenzyme and the surrounding residues. In particular, Glu370 plays an important role in the Co−C bond cleavage process. These effects tremendously enhance the stability of the Co−C bond cleavage state in the protein. The initial Co−C bond cleavage and the subsequent hydrogen transfer were found to occur in a stepwise manner in the protein, although the concerted pathway for the Co−C bond cleavage coupled with the hydrogen transfer is more favored in the gas phase. The assumed concerted transition state in the protein has more deformation of the coenzyme and the substrate and has less interaction with the protein than the stepwise route. Key factors and residues in promoting the enzymatic reaction rate have been discussed in detail.

1. Introduction

Methylmalonyl-CoA mutase (MMCM) is an important B_{12}-dependent enzyme that catalyzes a radical-based transformation of methylmalonyl-CoA to succinyl-CoA (Scheme 1).[1−3] A unique feature of this enzyme is the formation of a carbon-centered 5′-deoxyadenosyl (Ado) radical and a five-coordinated cob(II)alamin radical generated from homolytic cleavage of the Co−C bond of adenosylcobalamin (AdoCbl, step 1 in Scheme 2). The Ado radical then abstracts a hydrogen atom from the methylmalonyl-CoA substrate to generate a key intermediate, a substrate radical (step 2 in Scheme 2). The 1,2-rearrangement of the substrate can occur readily, only when the substrate radical is formed. Finally, the hydrogen transfer from the Ado moiety to the product radical followed by the reformation of the Co−C bond of the AdoCbl completes the full catalytic cycle.

Scheme 1. Conversion of Methylmalonyl-CoA to Succinyl-CoA by MMCM

Importantly, the reactivity of the first-step homolytic cleavage of the Co−C bond in the enzyme can be accelerated by a factor of 10^{12}, compared to that of the coenzyme in the aqueous solution.[1−3] In sharp contrast, the Co−C bond cleavage of AdoCbl is energetically unfavorable in the solution: (i) the Co−C bond dissociation energy (BDE) is ∼30 kcal/mol; (ii) the equilibrium constant for the Co−C bond homolysis is $\sim 8 \times 10^{-18}$ M; (iii) the rate constant for the bond cleavage was estimated to be $\sim 10^{-9}$ s^{-1}.[2,4,5] However, several B_{12}-dependent enzymes were found to promote the Co−C bond cleavage with the catalytic rates (k_{cat}) of ∼2−300 s^{-1}.[2,5,6] The equilibrium constant is close to unity in the enzymes.[2,4,6] In addition, the

[†] Kyoto University.
[‡] Technical University of Lodz.

(1) (a) Banerjee, R. *ACS Chem. Biol.* **2006**, *1*, 149. (b) Reed, G. H. *Curr. Opin. Chem. Biol.* **2004**, *8*, 477. (c) Banerjee, R. *Chem. Rev.* **2003**, *103*, 2083. (d) Banerjee, R.; Ragsdale, S. W. *Annu. Rev. Biochem.* **2003**, *72*, 209. (e) Toraya, T. *Chem. Rev.* **2003**, *103*, 2095. (f) Randaccio, L.; Geremia, S.; Wuerges, J. *J. Organomet. Chem.* **2007**, *692*, 1198. (g) Ludwig, M. L.; Matthews, R. G. *Annu. Rev. Biochem.* **1997**, *66*, 269. (h) Vlasie, M. D.; Banerjee, R. *J. Am. Chem. Soc.* **2003**, *125*, 5431. (i) Marsh, E. N.; Drennan, C. L. *Curr. Opin. Chem. Biol.* **2001**, *5*, 499. (j) Chowdhury, S.; Banerjee, R. *Biochemistry* **2000**, *39*, 7998. (k) Thomä, N. H.; Evans, P. R.; Leadlay, P. F. *Biochemistry* **2000**, *39*, 9213. (l) Babior, B. M. *Acc. Chem. Res.* **1975**, *8*, 376. (m) Banerjee, R., Ed. *Chemistry and Biochemistry of B12*; Wiley: New York, 1999. (n) Toraya, T. *Cell. Mol. Life Sci.* **2000**, *57*, 106.

(2) (a) Brown, K. L. *Chem. Rev.* **2005**, *105*, 2075. (b) Pratt, J. M. In *Handbook on Metalloproteins*; Bertini, I., Sigel, A., Sigel, H., Eds.; Marcel Dekker: New York, 2001; p 603. (c) Brown, K. L. *Dalton Trans.* **2006**, 1123. (d) Kratky, C.; Gruber, C. *Handbok of Metalloproteins*; Wiley: New York, 2001; pp 983−994, and references therein.

(3) (a) Riordan, C. G. In *Comprehensive Coordination Chemistry II*; Que, L., Jr.; Tolman, W. B., Eds.; Elsevier: Oxford, 2004; Vol. 8, p 677. (b) Marzilli, L. G. In *Bioinorganic Catalysis*; Reedijk, J., Bouwman, E., Eds.; Marcel Dekker: New York, 1999; p 423, and references therein.

Scheme 2. Formation of an Ado Radical (Step 1) and Hydrogen Transfer from the Substrate to the Ado Radical (Step 2) in MMCM

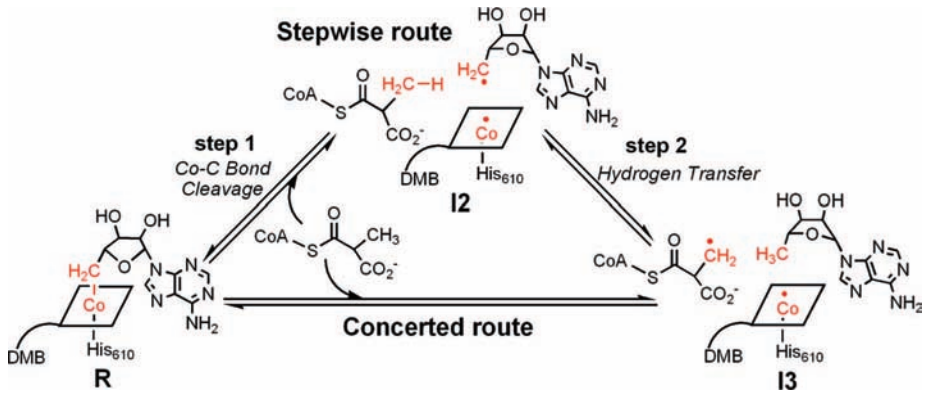

homolytic bond cleavage is found to be kinetically coupled to the hydrogen transfer from the substrate in these enzymes.[1,2,6]

The origin of these large catalytic enhancements is of great importance and significant interest and has been extensively studied. There are several different mechanistic explanations. The earliest one is the so-called mechanochemical trigger mechanism. The Co−N_{IM} bond was proposed to be compressed by the enzyme, which leads to upward folding of the corrin ring and to strain the Co−C bond.[7] However, recent theoretical and experimental investigations did not support this proposal.[8] As a matter of fact, it is difficult to experimentally determine the catalytic origin and quantify energy contributions from different factors. Consequently, the large catalytic effect in B_{12}-dependent enzymes has been the subject of debate and still remains an open issue. On the other hand, the detail of the hydrogen transfer process is poorly understood, although the stepwise route is generally believed (Scheme 2). However, a concerted route has recently been proposed.[2a,6b]

Recently, several groups performed the density functional theory (DFT) calculations or quantum mechanics/molecular mechanics (QM/MM)[9] investigations to explore the Co−C bond cleavage and its catalytic origin in B_{12}-dependent enzymes [MMCM and glutamate mutase (GluMut)].[10−12] Jensen and Ryde performed DFT and QM/MM calculations to study the Co−C bond cleavage in GluMut, which catalyzes rearrangement of glutamate to methylaspartate. The calculated Co−C bond dissociation energy was found to be significantly reduced, by as much as ∼32 kcal/mol, in the enzyme.[10d] Our groups also investigated the Co−C bond homolytic cleavage of MMCM by DFT and ONIOM calculations and by including an important part of the protein. The Co−C bond cleavage transition state in the protein was located for the first time.[11] A large conformational change of the ribose has been found to take place during the homolysis.[11] Meanwhile, Warshel et al. used the empirical valance bond (EVB) method and the free energy perturbation approach to examine the catalytic effect in MMCM. The catalytic effect was proposed to originate mainly from the electrostatic interaction between the ribose and the protein, instead of the strain effect of the coenzyme.[10c]

The hydrogen transfer step was briefly studied by Ryde.[10d] Very recently, the concerted and stepwise pathways for the Co−C bond homolysis and hydrogen transfer were theoretically examined for the first time by using a truncated model of the GluMut substrate in the gas phase. Kozlowski and Yoshizawa showed that the concerted route is lower in energy than the stepwise route by ∼7.0 kcal/mol.[10b] Warshel also showed that the concerted mechanism in MMCM was more favorable in the EVB simulations.[10c] Banerjee, Paneth and co-workers performed QM/MM simulations with semiempirical AM1 as the QM method to study the significant kinetic isotope effect in the stepwise hydrogen transfer step in MMCM.[10a,k]

The above two proposals, (*i*) the concerted Co−C bond cleavage and hydrogen transfer[10b] and (*ii*) the electrostatic origin

(4) (a) Hay, B. P.; Finke, R. G. *J. Am. Chem. Soc.* **1986**, *108*, 4820. (b) Finke, R. G.; Hay, B. P. *Polyhedron* **1988**, *7*, 1469. (c) Brown, K. L.; Zou, X. *J. Inorg. Biochem.* **1999**, *77*, 185.
(5) Finke, R. G. In *Vitamin B12 and the B12 proteins*; Kräutler, B., Arigoni, D., Golding, B. T., Eds.; Wiley-VCH: Weinheim, 1998; pp 383−402.
(6) (a) Padmakumar, R.; Padmakumar, R.; Banerjee, R. *Biochemistry* **1997**, *36*, 3713. (b) Buckel, W.; Golding, B. T.; Kratky, C. *Chem.—Eur. J.* **2006**, *12*, 352. (c) Pratt, J. M. In *Chemistry and Biochemistry of B12*; Banerjee, R., Ed.; Wiley: New York, 1999; pp 113−164. (d) Licht, S. S.; Booker, S.; Stubbe, J. *Biochemistry* **1999**, *38*, 1221. (e) Chih, H.-W.; Marsh, E. N. G. *Biochemistry* **1999**, *38*, 13684. (f) Meier, T. W.; Thoma, N. H.; Leadlay, P. F. *Biochemistry* **1996**, *35*, 11791. (g) Brown, K. L.; Li, J. *J. Am. Chem. Soc.* **1998**, *120*, 9466. (h) Licht, S. S.; Lawrence, C. C.; Stubbe, J. *Biochemistry* **1999**, *38*, 1234. (i) Marsh, E. N. G.; Ballou, D. P. *Biochemistry* **1998**, *37*, 11864.
(7) (a) Halpern, J. *Science* **1985**, *227*, 869. (b) Hill, H. A. O.; Pratt, J. M.; Williams, R. J. P. *Chem. Br.* **1969**, *5*, 169.
(8) (a) Jensen, K. P.; Ryde, U. *J. Mol. Struct.* **2002**, *585*, 239. (b) Sirovatka, J. M.; Rappe, A. K.; Finke, R. G. *Inorg. Chim. Acta* **2000**, *300*, 545. (c) Dong, S. L.; Padmakumar, R.; Banerjee, R.; Spiro, T. G. *J. Am. Chem. Soc.* **1999**, *121*, 7063. (d) Brooks, A. J.; Vlasie, M.; Banerjee, R.; Brunold, T. C. *J. Am. Chem. Soc.* **2005**, *127*, 16522. (e) Dölker, N.; Maseras, F.; Lledos, A. *J. Phys. Chem. B* **2001**, *105*, 7564. (f) Scheuring, E.; Padmakumar, R.; Banerjee, R.; Chance, M. R. *J. Am. Chem. Soc.* **1997**, *119*, 12192.
(9) Warshel, A.; Levitt, M. *J. Mol. Biol.* **1976**, *103*, 227.
(10) (a) Dybala-Defratyka, A.; Paneth, P.; Banerjee, R.; Truhlar, D. G. *Proc. Natl. Acad. Sci. U.S.A.* **2007**, *104*, 10774. (b) Kozlowski, P. M.; Kamachi, T.; Toraya, T.; Yoshizawa, K. *Angew. Chem., Int. Ed.* **2007**, *46*, 980. (c) Sharma, P. K.; Chu, Z. T.; Olsson, M. H. M.; Warshel, A. *Proc. Natl. Acad. Sci. U.S.A.* **2007**, *104*, 9661. (d) Jensen, K. P.; Ryde, U. *J. Am. Chem. Soc.* **2005**, *127*, 9117. (e) Dölker, N.; Maseras, F.; Siegbahn, P. E. M. *Chem. Phys. Lett.* **2004**, *386*, 174. (f) Freindorf, M.; Kozlowski, P. M. *J. Am. Chem. Soc.* **2004**, *126*, 1928. (g) Kozlowski, P. M.; Zgierski, M. Z. *J. Phys. Chem. B* **2004**, *108*, 14163. (h) Kuta, J.; Patchkovskii, S.; Zgierski, M. Z.; Kozlowski, P. M. *J. Comput. Chem.* **2006**, *27*, 1429. (i) Loferer, M. J.; Webb, B. M.; Grant, G. H.; Liedl, K. R. *J. Am. Chem. Soc.* **2003**, *125*, 1072. (j) Banerjee, R.; Truhlar, D. G.; Dybala-Defratyka, A.; Paneth, P. In *Hydrogen Transfer Reactions*; Hynes, J. T., Klinman, J. P., Limbach, H.-H., Schowen, R. L., Eds.; Wiley: Weinheim, 2007; pp 1473−1495. (k) Banerjee, R.; Dybala-Defratyka, A.; Paneth, P. *Philos. Trans. R. Soc. London, Ser. B* **2006**, *361*, 1333. (l) Dybala-Defratyka, A.; Paneth, P. *J. Inorg. Biochem.* **2001**, *86*, 681. (m) Rovira, C.; Kozlowski, P. M. *J. Phys. Chem. B* **2007**, *111*, 3251. (n) Kozlowski, P. M.; Andruniow, T.; Jarzecki, A. A.; Zgierski, M. Z.; Spiro, T. G. *Inorg. Chem.* **2006**, *45*, 5585. (o) Jensen, K. P.; Ryde, U. *J. Phys. Chem. A* **2003**, *107*, 7539. (p) Andruniow, T.; Zgierski, M. Z.; Kozlowski, P. M. *J. Am. Chem. Soc.* **2001**, *123*, 2679. (q) Brown, K. L.; Marques, H. M. *THEOCHEM* **2005**, *714*, 209. (r) Brown, K. L.; Marques, H. M. *J. Inorg. Biochem.* **2001**, *83*, 121, and references therein.
(11) Kwiecien, R. A.; Khavrutskii, I. V.; Musaev, D. G.; Morokuma, K.; Banerjee, R.; Paneth, P. *J. Am. Chem. Soc.* **2006**, *128*, 1287.

of the protein effect,[10c,13] are interesting. However, several questions remain to be answered for the enzymatic reaction mechanism. Is the proposed concerted pathway for the GluMut in the gas phase also operating in MMCM, when the methylmalonyl-CoA substrate and the protein are employed (Scheme 2)? Does the more accurate ONIOM(DFT/AMBER) method support the electrostatic effect and the concerted pathway in MMCM found by the EVB model? What are the main energetic and structural features for the Co−C bond cleavage and the hydrogen transfer processes in MMCM? Which residues play an important role in the protein effect of MMCM? In continuation of our efforts to answer these key issues on the Co−C bond cleavage in MMCM,[11] we have performed systematic and extensive DFT and ONIOM(DFT/AMBER) calculations with inclusion of a very large fraction of the MMCM protein. In this work, we will show that the coenzyme in the bound state has a relatively large strain in the protein, and the Co−C bond cleavage state can be stabilized by the release of the strain as well as the larger interaction with the nearby residues, particularly Glu370. Therefore, the Co−C bond cleavage is much easier in the protein than in the gas phase. In addition, our present calculations support the stepwise pathway for the Co−C bond cleavage and the subsequent hydrogen transfer in the protein, although the concerted pathway is more favorable in the gas phase.

2. Computational Methods and Model Systems

2.1. Setup of the System and Molecular Mechanics Calculations. All calculations in this work are based on the crystal structure of PDB entry 4REQ.[14] In the present work, residues 38−728 of chain A, the coenzyme, the truncated substrate,[11] and the corresponding crystal water molecules closer to chain A were included, while the remaining flexible residues 3−37 of chain A, which are very far away from the reaction center and interact with chain B, are not included in our calculations. Hydrogen atoms were added to the protein, presuming the normal protonation states of all titratable residues at the experimental pH (7.5) on the basis of the results of H++[15] and PROPKA[16] programs. In addition, the protonation states of histidine residues were assigned based on the visual inspection of the local protein environment. The charged protein with crystallographic water molecules was neutralized with sodium ions and fully solvated in a truncated octahedron water box constructed from a cubic box of 91.37 Å.

All molecular mechanics (MM) calculations have been performed with an AMBER all-atom force field and TIP3P water model.[17] The cobalamin AMBER parameters were taken from the literature.[18] As the AMBER force field is derived from RESP charges calculated at the HF/6−31G(d) level, we have also used the same approach to calculate RESP charges for the truncated substrate [Table S1 in the Supporting Information (SI)]. The bond, angle, and torsional parameters of the substrate are adapted from our previous work.[11] The MM optimization was carried out by the AMBER program.[19] The water molecules and counterions were first optimized. Afterward, the entire system with the Co−C5′ distance fixed was optimized to remove close contacts. Herein, the nonbonded cutoff radius was set to 12 Å. To reduce the computational cost for ONIOM calculations, the size of the entire system had to be reduced. Therefore, the MM-optimized structure, in which the solvation box and counterions introduced by the AMBER Leap module were removed, was taken as the initial geometry for the subsequent ONIOM optimizations.[20] Thus, the entire system consists of 12 033 atoms for our ONIOM calculations.

2.2. QM and ONIOM Hybrid Calculations. All QM and ONIOM calculations were carried out with the Gaussian program.[21] The (U)BP86/6−31G* (5d) method was used for all QM calculations.[22] In general, we used unrestricted (U) singlet calculations; these gave a closed-shell state, except for biradicaloid species where they led to open-shell "singlet" states. The nature of all minima and transition states was characterized by frequency calculations at the same level.

The ONIOM calculations have been performed with the use of a two-layer ONIOM (QM/MM) scheme,[23,24] in which the interface between the QM and MM regions is treated by hydrogen link atoms.[25] The total energy of the system is calculated by the following equation:

(12) Recent theoretical studies on rearrangement step in B12-dependent mutases: (a) Sandala, G. M.; Smith, D. M.; Marsh, E. N. G.; Radom, L. *J. Am. Chem. Soc.* **2007**, *129*, 1623. (b) Sandala, G. M.; Smith, D. M.; Radom, L. *J. Am. Chem. Soc.* **2006**, *128*, 16004. (c) Sandala, G. M.; Smith, D. M.; Coote, M. L.; Golding, B. T.; Radom, L. *J. Am. Chem. Soc.* **2006**, *128*, 3433. (d) Wetmore, S. D.; Smith, D. M.; Bennett, J. T.; Radom, L. *J. Am. Chem. Soc.* **2004**, *126*, 14054. (e) Wetmore, S. D.; Smith, D. M.; Bennett, J. T.; Radom, L. *ChemBioChem* **2001**, *2*, 919. (f) Wetmore, S. D.; Smith, D. M.; Golding, B. T.; Radom, L. *J. Am. Chem. Soc.* **2001**, *123*, 7963. (g) Kamachi, T.; Toraya, T.; Yoshizawa, K. *Chem.−Eur. J.* **2007**, *13*, 7864. (h) Kamachi, T.; Toraya, T.; Yoshizawa, K. *J. Am. Chem. Soc.* **2004**, *126*, 16207, and references therein.

(13) Warshel, A.; Sharma, P. K.; Kato, M.; Xiang, Y.; Liu, H. B.; Olsson, M. H. M. *Chem. Rev.* **2006**, *106*, 3210.

(14) Mancia, F.; Evans, P. R. *Structure* **1998**, *6*, 711.

(15) H++: http://biophysics.cs.vt.edu/H++. A server for estimating pK_a's and adding missing hydrogens to macromolecules: (a) Gordon, J. C.; Myers, J. B.; Folta, T.; Shoja, V.; Heath, L. S.; Onufriev, A. *Nucleic Acids Res.* **2005**, *33*, 68–71 (Web Server issue), *W3*. (b) Bashford, D.; Karplus, M. *Biochemistry* **1990**, *29*, 10219.

(16) Li, H.; Robertson, A. D.; Jensen, J. H. *Proteins: Struct., Funct., Bioinf.* **2005**, *61*, 704.

(17) (a) Cornell, W. D.; Cieplak, P.; Bayly, C. I.; Gould, I. R.; Merz, K. M., Jr.; Ferguson, D. M.; Spellmeyer, D. C.; Fox, T.; Caldwell, J. W.; Kollman, P. A. *J. Am. Chem. Soc.* **1995**, *117*, 5179. (b) Jorgensen, W. L.; Chandrasekhar, J.; Madura, J. D.; Impey, R. W.; Klein, M. L. *J. Comput. Phys.* **1983**, *79*, 926.

(18) (a) Marques, H. M.; Ngoma, B.; Egan, T. J.; Brown, K. L. *J. Mol. Struct.* **2001**, *561*, 71. (b) Marques, H. M.; Brown, K. L. *THEOCHEM* **1995**, *340*, 97.

(19) Case, D. A. et al. *AMBER 8*; University of California: San Francisco, 2004.

(20) Classical MD simulations to relax this large MMCM protein were suggested by one of the referees. However, the reaction barrier was found to be influenced by the MD snapshots (Zhang, Y.; Kua, J.; McCammon, J. A. *J. Phys. Chem. B* **2003**, *107*, 4459.). The computational costs to perform our systematic ONIOM calculations with the large QM models and different MD snapshots are prohibitively high.

(21) Frisch, M. J. et al. Gaussian Development Version, G.01 and G.03; Gaussian, Inc.: Wallingford, CT, 2007.

(22) (a) Becke, A. D. *J. Chem. Phys.* **1986**, *84*, 4524. (b) Perdew, J. P. *Phys. Rev. B* **1986**, *33*, 8822.

(23) (a) Maseras, F.; Morokuma, K. *J. Comput. Chem.* **1995**, *16*, 1170. (b) Humbel, S.; Sieber, S.; Morokuma, K. *J. Chem. Phys.* **1996**, *105*, 1959. (c) Matsubara, T.; Sieber, S.; Morokuma, K. *Int. J. Quantum Chem.* **1996**, *60*, 1101. (d) Svensson, M.; Humbel, S.; Froese, R. D. J.; Matsubara, T.; Sieber, S.; Morokuma, K. *J. Phys. Chem.* **1996**, *100*, 19357. (e) Svensson, M.; Humbel, S.; Morokuma, K. *J. Chem. Phys.* **1996**, *105*, 3654. (f) Dapprich, S.; Komáromi, I.; Byun, S.; Morokuma, K.; Frisch, M. J. *THEOCHEM* **1999**, *461*, 1. (g) Vreven, T.; Morokuma, K. *J. Comput. Chem.* **2000**, *21*, 1419. (h) Vreven, T.; Byun, K. S.; Komáromi, I.; Dapprich, S.; Montgomery, J. A., Jr.; Morokuma, K.; Frisch, M. J. *J. Chem. Theory Comput.* **2006**, *2*, 815.

(24) (a) A new quadratic coupled algorithm was used in all ONIOM calculations. All transition states were fully optimized by this new optimization algorithm implemented in the Gaussian Development version: Vreven, T.; Frisch, M. J.; Kudin, K. N.; Schlegel, H. B.; Morokuma, K. *Mol. Phys.* **2006**, *104*, 701. (b) By default, there is no cutoff for MM nonbonded terms in the Gaussian code.

(25) (a) Singh, U. C.; Kollman, P. A. *J. Comput. Chem.* **1986**, *7*, 718. (b) Field, M. J.; Bash, P. A.; Karplus, M. *J. Comput. Chem.* **1990**, *11*, 700.

$$E_{ONIOM}=E_{MM,real} + E_{QM,model} - E_{MM,model} \quad (1)$$

Herein, $E_{MM,real}$ is the MM energy of the entire system, called the real system. $E_{QM,model}$, denoted by E_{QM} later in this study, is the QM energy of the model system, a chemically important part of the real system. $E_{MM,model}$ is the MM energy of the model system. Electrostatic interactions between the QM and MM layers were calculated by a mechanical embedding scheme.[23] The protein effect can be evaluated as follows: $\Delta E_{MM} = \Delta E_{MM,real} - \Delta E_{MM,model}$. In the present ONIOM optimization calculations, the (U)BP86/6−31G* (5d) method and AMBER force field[17] are employed as the high-level QM method and the low-level MM method, respectively. The real system was further divided into the optimized MM region and the frozen MM region.[10d,26] The residues within ~10 Å of any QM atom of the coenzyme and the substrate were assigned to the optimized MM region and allowed to be optimized. In this work, several QM models have been used to investigate the Co−C bond cleavage and the subsequent hydrogen transfer. The MMCM structure for our ONIOM calculations and the partition of the QM and MM regions are depicted in Scheme 3. The smallest QM model, M1, consists of 74 QM atoms, while the largest QM model (M6) contains 119 QM atoms.[27] The energies discussed in our study are relative electronic energies unless specifically noted.

3. Results and Discussion

The detailed protein effect on the initial Co−C bond cleavage in MMCM was not investigated in our previous study.[11] We first summarize important results of our current QM and ONIOM calculations by adopting the simplest QM system of M1 (section 3.1). Key results by using the other four larger QM models (M2-M5) on the Co−C bond cleavage process are then discussed (section 3.2). Finally, the feasibility of the concerted and stepwise pathways for the Co−C bond cleavage process and hydrogen transfer will be presented in section 3.3. The detailed results and discussion were also collected in SI.

3.1. Co−C Bond Cleavage (M1). 3.1.1 Co−C Bond Cleavage in the Gas Phase. The optimized Co−C5′ bond length of the coenzyme in the gas phase is 2.01 Å, which is in good agreement with the corresponding distance of 2.03 Å in the crystal structure of AdoCbl.[28] We studied the Co−C5′ bond cleavage process by optimizing the coenzyme with varying the Co···C5′ distances (2.0−4.0 Å) and by fully optimizing the completely dissociated products. The relaxed potential energy surface (PES) scan (i.e., with geometries optimized at each fixed value of Co−C distance) in the gas phase in Figure 1 shows that the bond dissociation takes place without a transition state. The calculated BDE value of the Co−C bond, the energy difference between the completely dissociated radical fragments and the most stable Co−C bound state, is 38.0 [without zero-point energy correction (ZPC)] and 33.6 kcal/mol (with ZPC), which is consistent with the experimental value.[2,4,5] These results suggest that the present model is appropriate in describing the bond cleavage step. The spin densities of Co and C5′ in the gas phase are shown in Figure S1.[29a]

3.1.2. Co−C Bond Cleavage in MMCM. We also studied the Co−C bond breaking step in the protein (Figure 1). The PES (without ZPC) in the protein significantly differs from that in the gas phase. Namely, in the protein, the Co−C bond breaking reaction takes place with a barrier at the homolytic cleavage transition state $\mathbf{TS_{I1-I2}}$. The barrier relative to the most stable Co^{III} state **R** is 17.3 kcal/mol, and the BDE from **R** to the Co−C bond cleavage state **I2** is 9.8 kcal/mol. This BDE is dramatically decreased from 38.0 kcal/mol in the gas phase, as discussed before.[30] Consequently, the enzyme is calculated to lower the bond cleavage barrier by 20.7 kcal/mol and reduce the BDE by 28.2 kcal/mol to give **I2**, compared to the dissociation in the gas phase.[29b] These results are qualitatively in line with the observed catalytic effect and the energy of reaction for the Co−C bond cleavage step.

As shown in eqs S1−S4 in the SI, the catalytic effect of protein in the energetics can be categorized into three major terms: cage effect, structural distortion of the QM coenzyme, and MM energy contribution. The cage effect comes from the fact the protein does not allow the Ado radical to fully dissociate from the coenzyme. The Co···C5′ distance of **I2** in the protein is ~4.0 Å. In the gas phase, as shown in Figure 1, the energy cost to elongate the Co−C bond to 4.0 Å is 32.6 kcal/mol, while that (i.e., BDE) to completely dissociate the products is 38.0 kcal/mol. This energy difference, 5.4 kcal/mol, is sometimes called the cage effect in the protein, which is due to the interaction between the OH groups of the ribose and the corrin ring.[10d,e] The remaining protein effects, the QM contribution (i.e., structural distortion of the QM coenzyme) and the MM energy contribution (including the interaction between QM and MM parts), were shown in Table 1.[31]

For the QM contribution, the QM model is more destabilized by approximately 5.5 kcal/mol for **R** and 15.9 kcal/mol for **I1** in the protein, compared to the gas phase. Therefore, the energy of reaction in terms of ΔE_{QM} to give **I2** becomes less endothermic in the protein, due to more structural distortion of the QM model part (the major part of the coenzyme) caused by the protein in **R** and **I1**. For the MM contribution, **R** and **I1** are less stable than **I2** by 17.3 and 17.8 kcal/mol, respectively. The origin of the QM contribution and the MM energy contribution will be discussed in the following two subsections.

3.1.3. QM Contribution: Structural Distortion of the Coenzyme. The geometric distortion of the coenzyme[32] can be reflected by the key structural parameters of the ONIOM-optimized **R**, **I1**, $\mathbf{TS_{I1-I2}}$, and **I2**, as shown in Table 2 as well as in Figure 2 and Table S4. Proceeding from **R** to **I2**, considerable conformational change of the Ado moiety is found to involve gradual changes of the following geometrical

(26) Altun, A.; Shaik, S.; Thiel, W. *J. Comput. Chem.* **2006**, *27*, 1324.
(27) One of the referees suggested performing calculations with the largest QM model (without MM atoms) and ONIOM calculations with approximately 70 QM and 50 MM atoms to check the reliability of the ONIOM method. However, interactions between the QM and MM parts are described by the classical mechanics in the latter case. In addition, by using such a small and flexible system, the results should be less realistic than the real protein system.
(28) Ouyang, L.; Rulis, P.; Ching, W. Y.; Nardin, G.; Randaccio, L. *Inorg. Chem.* **2004**, *43*, 1235.
(29) (a) The diradical character of the coenzyme starts to appear at the Co−C bond length of ~2.7 Å and increases with the Co−C bond distance in the gas phase. (b) Spin density analysis verifies that the Co−C bond cleavage is homolytic and the diradical character of the coenzyme begins at the Co−C bond length of ~2.6 Å, slightly shorter than the gas phase (Figure S1). Also, more diradical character is found in the protein, indicating that homolytic cleavage is promoted by the protein.
(30) **I1** is a metastable Co^{III} state, which was located previously together with $\mathbf{TS_{I1-I2}}$ (ref 11). **I1** is higher in energy than **I2** by 1.1 kcal/mol. There is a large geometrical change between **R** and **I1**. The conversion process between **R** and **I1** was unclear in the previous study. Such isomerization has been investigated and discussed in the Supporting Information.
(31) The MM energy contribution in Table 1 includes the interaction of the QM model part with the MM part of the coenzyme and the surrounding protein, as well as the internal energy difference of the protein between the Co^{III} and Co^{II} states. Relative contribution from the MM part of the coenzyme is also shown in Table S2 of the Supporting Information.

Scheme 3. Structure for Our ONIOM Calculations and Partition of QM and MM Regions

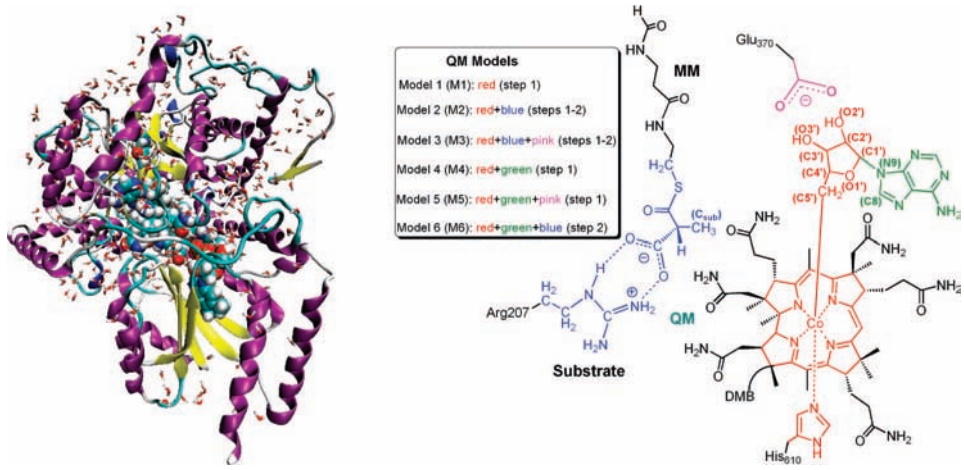

parameters: θ(C5′−C4′−C3′−C2′), X_{CN}(O1′−C1′−N9−C8) (exocyclic ribose dihedral angle), P, and θ_m (pseudorotation phase and amplitude).[33a,b] For instance, the ribose adopts an O1′-endo conformation with more puckering in **R**, while it adopts a C1′-endo conformation with less puckering in **I2**, which is consistent with the X-ray crystal structure of 4REQ.[14] Similarly, pseudorotation of the ribose has been found in X-ray crystal structures of GluMut,[34] which supports the conformational changes of the Ado moiety. Our group also showed that the reaction barrier of the pseudorotation of the ribose in the gas phase is very low.[33a] Moreover, the Co^{III} states (**R** and **I1**) have a much larger Co−C5′−C4′ angle in the protein (∼140°) than that in the gas phase (124°) and the Co^{II} state in the protein (121°). In fact, the B_{12} enzymes were suggested to activate the Co−C bond by altering the Co−C5′−C4′ bond angle.[8c,10d] Consequently, the metastable Co^{III} state **I1** has high strain energy coming from the ribose (Table S3). Interestingly, **R** has a strain energy higher than that of **I2** by ∼5.5 kcal/mol. The strain partly caused from the Co−C5′−C4′ bond angle in **R** is compensated by relieving some of the strain in the ribose through the pseudorotation,[33a] which also strengthens the Co−C bond. As shown in Figure 2 and indicated by the dihedral angle θ, the C5′ and the adenine are in favorable pseudoequatorial positions

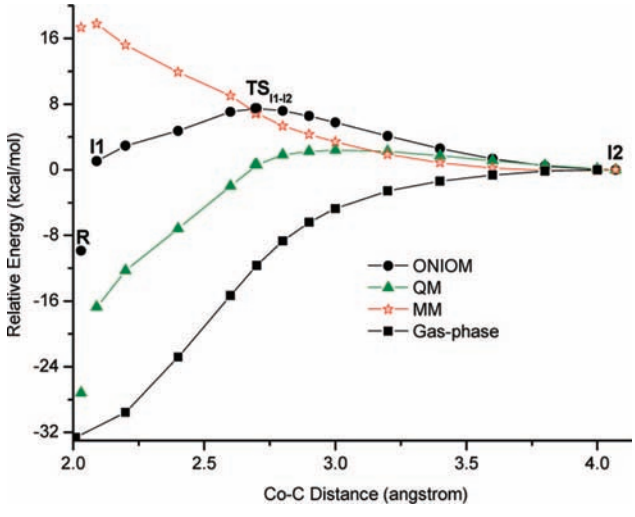

Figure 1. Potential energy surfaces (without ZPC) of the Co−C bond cleavage in the gas phase and in the protein. The energies in the protein are relative to the Co−C bond cleavage state **I2**. The energies in the gas phase are relative to the state at the Co−C distance of 4.0 Å (see text).

Table 1. Relative Energies (in kcal/mol, Compared to **I2**) of the ONIOM Calculations with M1 and M4 QM Models

	ΔE_{ONIOM}	ΔE_{QM}	ΔE_{MM}	$\Delta E_{Coulomb}$	ΔE_{vdw}	$\Delta E_{torsion}$
R (M1)	−9.8	−27.1	17.3	4.0	7.1	5.2
I1 (M1)	1.1	−16.7	17.8	3.3	5.2	8.4
$\mathbf{TS_{I1-I2}}$ (M1)	7.5	0.6	6.9	5.2	−2.1	2.5
R (M4)	−12.1	−21.4	9.3	2.6	4.5	1.2
I1 (M4)	−8.3	−18.0	9.7	4.2	3.7	1.3
$\mathbf{TS_{I1-I2}}$ (M4)	3.2	0.8	2.4	4.2	−2.5	0.6

Table 2. Selected Structural Parameters in the Coenzyme Optimized with ONIOM Using M1 QM Model[a]

	Co−C5′	$Co-N_{His610}$	Co−C5′-C4′	θ	X_{CN}	P	θ_m	ω
R	2.03	2.20	135.8	−163.6	−7.8	87.5	47.6	6.9
I1	2.09	2.27	140.7	−110.7	51.7	237.8	12.0	9.7
$\mathbf{TS_{I1-I2}}$	2.70	2.26	141.2	−125.3	54.1	284.7	18.6	7.0
I2	4.07	2.13	121.0	−127.8	64.1	311.7	27.9	7.7

[a] Bond lengths and angles are in Å and degree, respectively.

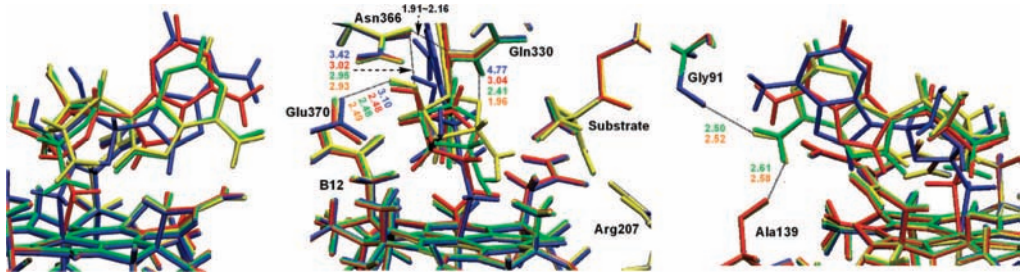

Figure 2. Superimposition of the ONIOM-optimized structures of **R** (blue), **I1** (red), $\mathbf{TS_{I1-I2}}$ (green), and **I2** (yellow) for M1 in the protein. Some important distances are also shown in Å.

in **R**, but they are in pseudoaxial positions during the cleavage process (**I1**, $\mathbf{TS_{I1-I2}}$, and **I2**).

3.1.4. MM Energy Contribution. The MM energy contribution in the protein can be further partitioned into Coulomb, van der Waals, stretching, bending, torsion, and out-of-plane energy terms. As shown in Figure S3, Coulomb, van der Waals, and torsion terms are found to be the major contributors to the protein MM effect. As listed in Tables 1 and S2, the MM energy, ΔE_{MM} relative to **I2**, is decreased from the Co^{III} state (**R** or **I1**) to $\mathbf{TS_{I1-I2}}$. Moreover, most torsion energies and part of the van der Waals energies arise from the coenzyme, while part of the van der Waals energies and most Coulomb energies are attributed to the other residues around the coenzyme. In addition, electrostatic and van der Waals contributions of various protein residues (Figures S4 and S5) are related to the hydrogen bonding networks seen in Figure 2. Several key residues are found to stabilize **I2** more than **R**, mainly due to hydrogen bonds. For instances, Gln330 forms a hydrogen bond with the O1′ of the ribose in **I2** ($NH_{Gln330}\cdots O1'_{ribose}$: 1.96 Å vs 4.77 Å in **R**).[35] Glu370 also has a hydrogen bond with the O2′H group of the ribose in **I2** ($O_{Glu370}\cdots HO2'_{ribose}$: 2.49 Å vs 3.10 Å in **R**). This supports the interaction between Glu370 and the ribose OH group playing a crucial role in the electrostatic catalysis in MMCM.[10c] In one word, our results shown in Figures S3−S5 indicate that the electrostatic and van der Waals interactions of the nearby residues with the Ado moiety in **I2** are responsible for making Co−C bond cleavage easier in the protein than in the gas phase. A similar observation was also found in the theoretical study on another B_{12}-dependent GluMut.[10d]

3.2. Effects of Substrate, Arg207, Glu370, and Adenine on the Co−C Bond Cleavage in MMCM (M2−M5). The QM effects of the substrate, key residues (Arg207 and Glu370), and the adenine base on the Co−C bond cleavage were further explored by using larger QM models M2−M5 (Scheme 3). The QM effect of the substrate and Arg207, both in energetics and geometry, in M2 was found to be very small (Figures S6−S8 and Tables S5−S6), whereas the QM effects of Glu370 in M3 and M5, as well as the adenine base in M4 and M5, are quite pronounced. Therefore, we mainly discuss key results of the QM effects of the adenine base and Glu370 for M4 and M5. The detailed results and discussion for M2 and M3 are given in the SI.

As discussed before, the Co^{III} states have the large torsion energy mainly from the MM part of the coenzyme (Table S2). Relative to $\mathbf{TS_{I1-I2}}$ and **I2**, some displacement of the adenine may stem from the torsion strain in the crowded bound states **R** and **I1** (see Figure 2). Hence, we further explored its QM

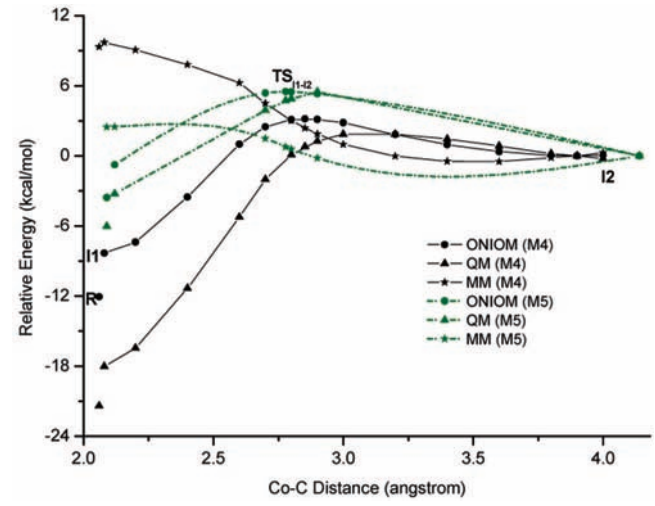

Figure 3. Potential energy profiles of the Co−C bond cleavage in the protein calculated for M4 (black lines) and M5 (green lines) in the protein. The energies are relative to the Co−C bond cleavage state.

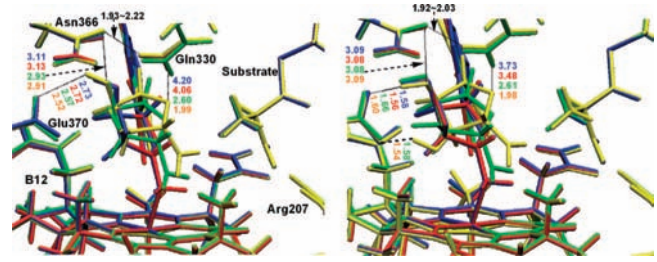

Figure 4. Superimposition of the ONIOM-optimized structures of **R** (blue), **I1** (red), $\mathbf{TS_{I1-I2}}$ (green), and **I2** (yellow) calculated for M4 (left) and M5 (right) in the protein. Some important distances are also shown in Å.

effect on the Co−C bond cleavage using M4 and M5 in Scheme 3 (Figures 3, 4, S8 and Tables S3−S6). Interestingly, optimization of **I1** (Co−C: 2.08 Å) gives a structure with an Ado conformation very similar to that in **R** (Co−C: 2.06 Å), albeit the position of the adenine is slightly different. As a result, **R** and **I1** are close in energy. The interconversion between **R** and **I1** should be regarded as being very facile and the PES for the Co−C bond cleavage should become essentially continuous (Figures S10),[36] when the large QM coenzyme is used. In going from M1 to M4, ΔE_{MM} of **R** decreases from 17.3 to 9.3 kcal/mol and $\Delta E_{torsion}$ for the MM part of the coenzyme is reduced from 4.7 to 0.4 kcal/mol (Tables 1 and S2). These results support the main MM torsion in M1 originating from the adenine. At the same time, when this torsion is treated by the QM method, ΔE_{QM} of **R** increases from −27.1 kcal/mol for M1 to −21.4 kcal/mol for M4.[37] Collectively, the stability of **R**, in terms of ΔE_{ONIOM}, is slightly increased by about 2.3 kcal/mol for M4 relative to M1. These calculations also suggest that torsion of the adenine described by the MM method leads to an inappropriate structure **I1** (with the close contact between the hydrogen atoms on C5′ and C8 for M1−M3). Also, the torsion is overestimated by ∼2 kcal/mol. In addition, the reaction barrier

(32) (a) To further evaluate the strain energy of various fragments in the QM part of the coenzyme, we took the QM part of the coenzyme from the ONIOM calculations and then reoptimized the interested fragment (e.g., ribose) in the gas phase by freezing the rest of the coenzyme at the ONIOM-optimized geometry (ref 10d). The details and calculated strain energies of the QM coenzyme are tabulated in Table S3 and Scheme S1. (b) The QM contribution is found to be nearly equal to the strain energy difference between the Co^{III} and Co^{II} states induced by the protein.

(33) (a) Khoroshun, D. V.; Warncke, K.; Ke, S.-C.; Musaev, D. G.; Morokuma, K. *J. Am. Chem. Soc.* **2003**, *125*, 570. (b) Altona, C.; Sundaralingam, M. *J. Am. Chem. Soc.* **1972**, *94*, 8205. (c) Levitt, M.; Warshel, A. *J. Am. Chem. Soc.* **1978**, *100*, 2607. (d) Jensen, K. P.; Sauer, S. P. A.; Liljefors, T.; Norrby, P.-O. *Organometallics* **2001**, *20*, 550.

(34) Gruber, K.; Reitzer, R.; Kratky, C. *Angew. Chem., Int. Ed.* **2001**, *40*, 3377.

(35) Similarly, the N_ε atom of Arg66 could have some electrostatic attraction with the O1′ of the ribose ($N_{Arg66}\cdots O1'$: 3.37−3.41 Å) in GluMut, when the Co−C bond is completely broken (ref 34).

(36) The relaxed scan calculations starting from **R** showed that all energies, ΔE_{ONIOM}, ΔE_{QM}, and ΔE_{MM}, are very similar to those starting from **I2**, after the Co−C bond is considerably elongated (Figure S11).

(37) The strain energy difference of the QM part of the coenzyme between **R** and **I2** is slightly increased to 7.8 kcal/mol for M4 (Table S3). The QM contribution is almost equal to the strain energy difference between the Co^{III} and Co^{II} states induced by the protein.

via $\mathbf{TS_{I1-I2}}$ is slightly reduced to 15.3 kcal/mol for M4. As a whole, the QM effect of the adenine has some influence on the energetics and geometry of the Co−C bond cleavage process, particularly the Ado conformation in **I1**.

To assess the combined QM effects, M5 was created in which Glu370 was added into the QM region of M4. The PESs and optimized key structures for the Co−C bond cleavage are summarized in Figures 3, 4, S8 and Tables S3, S5−S6. Similar to M3, Glu370 is shown to activate the Co−C bond of the Co^{III} state by slightly elongating the Co−C bond to 2.09 Å in **R** and 2.12 Å in **I1**, due to the very strong hydrogen bonds between Glu370 and the ribose. Similar to M4, **R** and **I1** in M5 have a similar Ado conformation. Due to the formation of the very strong hydrogen bonds, both Co^{III} and Co^{II} states have larger strain energies as well as a larger strain energy difference between the two states for M5, compared to M4 (Table S3). The conformational change of the Ado was observed in **I2** for M5 (Figures 4 and S8). The significant QM effects of the adenine and Glu370 give rise to a much smaller ΔE_{QM} of −6.0 and −3.2 kcal/mol for **R** and **I1**, respectively, due to the reactant destabilization, smaller BDE of the Co−C bond, and larger interaction with Glu370 in **I2**. The protein MM effect is subsided to ∼2 kcal/mol. Combining both QM and MM effects, **R** and **I1** are calculated to be slightly lower in ΔE_{ONIOM} than **I2** by approximately 3.6 and 0.8 kcal/mol for M5.[38] In addition, the reaction barrier through $\mathbf{TS_{I1-I2}}$ computed for M5 is further reduced to 9.1 kcal/mol. These results show that Glu370 destabilizes the Co^{III} state via the Co−C bond elongation but stabilizes the Co−C bond cleavage state via stronger hydrogen bonding and, thus, electrostatic interaction with the ribose.

In summary, all ONIOM calculations using different QM models (M1−M5) qualitatively give similar PESs for the Co−C bond cleavage process and demonstrate a large catalytic effect of the protein. The large catalytic effect can be attributed to the cage effect, the larger geometrical deformation of the coenzyme (mainly from the Ado) in the bound state, the stronger interaction of the ribose with Glu370 in the Co−C bond cleavage state, and some contributions from the nearby residues (e.g., Gln330) via the Coulomb, van der Waals, and torsion interactions. The QM effects of the AdoCbl, via strain effect, and Glu370, via very strong hydrogen bonding, are dominant in the total protein effect in MMCM (i.e., M5, $\Delta E = 3.6$ kcal/mol and $\Delta E^{\ddagger} = 9.1$ kcal/mol). The energetics and geometry of the coenzyme in the bound state with the relatively large strain from the Ado are shown to be described better by the more accurate QM method.

Remarkably, the large enzymatic protein effect is not dominated by the strain effect in **R** (reactant destabilization), although the much larger Co−C5′−C4′ angle found in **R** was suggested to activate the Co−C bond.[8c,10d] The very flexible Ado utilized by MMCM is essential. The conformation of the Ado can be finely tuned during the Co−C bond cleavage process (Figure S10). The Ado moiety adopts an energetically more favorable conformation in the crowded **R**, which partly compensates the strain from the Ado and renders the shorter Co−C bond. When the Co−C bond is broken, the Ado moiety becomes more flexible to undergo the conformational change, which enhances the interaction of the Ado with the nearby residues, such as Glu370 and Gln330.[39] Also, the conformational change shuttles the C5′ radical closer to the substrate carbon for the hydrogen transfer or to the metal center.[34]

The very large protein effect on the Co−C bond cleavage in MMCM observed in our current work is qualitatively similar to the two previous studies on the B_{12}-dependent MMCM and GluMut,[10c,d] but some differences are also found. In the Warshel's EVB study on MMCM, the PES along the stepwise Co−C cleavage, which was calibrated from the RB3LYP calculations, was uphill even at 4 Å and its computed reaction free energy is ∼13 kcal/mol.[10c] In addition, the protein effect was almost all attributed to the electrostatic interaction of Glu370 and ribose. The concerted route, in which 10 kcal/mol of driving force for the hydrogen transfer step was introduced, was calculated to be more favorable than the stepwise Co−C cleavage.[10c] Interestingly, relatively similar to our study, Ryde concluded several factors including the cage effect (∼4.8 kcal/mol), the strain effect of the coenzyme (∼14.6 kcal/mol), the protein MM effect (∼10.0 kcal/mol, by electrostatic and van der Waals interactions), and the stabilized protein itself (∼2.6 kcal/mol) in the dissociated state as responsible for the catalytic effect in GluMut.[10d] However, interactions between Ado with nearby charged residues (Arg66, Glu330, and Lys326) in GluMut were evaluated by the MM method,[10d] which may underestimate critical interactions among these key parts (e.g., mutual polarization and charge transfer). Furthermore, the conformational change of the Ado during the Co−C bond cleavage has not been reported in these two works. Different from MMCM, the pseudorotation was found to occur after the Co−C cleavage to give one intermediate in GluMut.[34]

3.3. Stepwise and Concerted Pathways for the Co−C Bond Cleavage and Hydrogen Transfer (M2, M3, and M6). The details of the hydrogen transfer in MMCM are not very clear. We will discuss now which of the stepwise and concerted pathways for the Co−C bond cleavage and hydrogen transfer is more favorable in MMCM as well as in the gas phase and how the protein influences the hydrogen transfer.

3.3.1. Reaction Pathways in the Gas Phase. The key results of the concerted and stepwise pathways in the gas phase are summarized in Figures S12 and S13. The stepwise route starts with the Co−C bond cleavage, leading to the metal-centered cob(II)alamin radical and the carbon-centered ribose radical, which then abstracts a hydrogen atom from the substrate. The complexation energy to form complex **IIS** is 11.0 kcal/mol (9.4 kcal/mol with ZPC), due to hydrogen-bonding interactions. The reaction barrier for the stepwise hydrogen transfer via $\mathbf{TS_{IIS\text{-}IIIS}}$ is 18.2 kcal/mol (ZPC: 15.7 kcal/mol) relative to **IIS** and 55.0 kcal/mol (ZPC: 48.9 kcal/mol) relative to the lowest-energy complex **IC**. For the stepwise hydrogen transfer pathway, the cob(II)alamin radical, which is absent in **IIS**, **IIIS**, and $\mathbf{TS_{IIS\text{-}IIIS}}$, was regarded as a spectator.[10b]

For the concerted pathway, the calculated complexation energy to form complex **IC** is ∼9.8 kcal/mol (9.0 kcal/mol with ZPC). The concerted hydrogen transfer transition state $\mathbf{TS_{IC\text{-}IIIC}}$ is also much higher in energy, 46.7 kcal/mol (ZPC:

(38) Glu370 forms two strong intermolecular hydrogen bonds with the ribose in **I2**, while it forms one intermolecular hydrogen bond in **R** and **I1**. Also Co^{III} states **R′ and I1′** with two intermolecular hydrogen bonds are calculated to be comparable in energy. **R′** is only higher than **R** by 0.5 kcal/mol. **I′** is a little lower than **I1** by 0.1 kcal/mol (Figures S9).

(39) These important interactions in the closed and reactive form of MMCM may partly explain the very small protein effect in the unreactive form in our previous calculations (ref 11), as Glu370 and Gln330 cannot form hydrogen bonds with the ribose in the unreactive form. It should be noted that only one carboxylic oxygen of Glu247 was found to interact with the ribose. Therefore, stabilization on the dissociated state by the protein in the unreactive form should be less than the reactive form.

41.2 kcal/mol) above **IC**.[40] Similar to the GluMut model study in the gas phase,[10b] the concerted transition state $\mathbf{TS_{IC\text{-}IIIC}}$ is lower in energy than the stepwise hydrogen transfer transition state $\mathbf{TS_{IIS\text{-}IIIS}}$ by 8.3 kcal/mol (7.7 kcal/mol with ZPC).[41] Hence, the cob(II)alamin radical was considered as a conductor in the concerted path.[10b] In $\mathbf{TS_{IC\text{-}IIIC}}$, nearly one (negative) spin (spin density: −0.98) resides in the cobalt center, while one (positive) spin is delocalized over the two carbon centers (spin density of C5′ and C_{sub} is +0.53 and +0.50, respectively). Also, in $\mathbf{TS_{IIS\text{-}IIIS}}$, one spin is found to be delocalized over the two carbon centers (spin density of C5′ and C_{sub} is +0.55 and +0.51, respectively). The Co···C5′ bond distance in $\mathbf{TS_{IC\text{-}IIIC}}$ is very long. Interestingly, the stepwise transition state $\mathbf{TS_{IIS\text{-}IIIS}}$ and the concerted transition state $\mathbf{TS_{IC\text{-}IIIC}}$ have similar C5′···H and H···C_{sub} distances (∼1.3−1.4 Å, see Figure S13). In summary, the concerted pathway is more favorable than the stepwise route in the gas phase.

Deuterium kinetic isotope effects (D-KIEs) were calculated at the conventional transition theory level from the Bigeleisen equation[42] using the ISOEFF program.[43] In principle D-KIEs should be helpful in deciding whether a mechanism is stepwise or concerted. In the present case, however, the transition state structures that we were able to obtain, even for the most "concerted" cases, are extremely asynchronous with the C−Co distance never being shorter than 3.57 Å. A concerted mechanism involving such a transition state is in fact so close to a formally stepwise mechanism that distinguishing between these two alternative mechanisms is more semantic than practical. Nevertheless, the very large D-KIE observed experimentally[44] (∼50 at 5 °C) implies that the semiclassical value of D-KIE as well as the quantum correction for tunneling should be very large, probably at their theoretical limits. Our calculations indicate that both of these values are larger for stepwise pathways. Namely, semiclassical D-KIEs for concerted $\mathbf{TS_{IC\text{-}IIIC}}$ (as well as $\mathbf{TS'_{IC\text{-}IIIC}}$, and $\mathbf{TS''_{IC\text{-}IIIC}}$ in Figure S13) is under 7.0, while, for $\mathbf{TS_{IIS\text{-}IIIS}}$, the transition state of the second step of the stepwise mechanism, it is 7.3. Also one-dimensional Wigner quantum correction,[45] which is known to underestimate the contribution of tunneling, is largest in the case of the stepwise transition state. Thus we conclude that qualitatively D-KIEs calculated on the basis of present studies favor the stepwise mechanism.

3.3.2. Reaction Pathways in the Protein. The above calculations indicate that the concerted pathway is energetically favored in the gas phase. However, the protein interaction was not included and the cob(II)alamin is also present in the stepwise route in the protein, due to the cage effect. Here the effect of the protein on the stepwise and concerted routes was first studied by using M2.

Table 3. Relative Energies (in kcal/mol) for the Hydrogen Transfer Step in M2, M3, and M6

	ΔE_{ONIOM}	ΔE_{QM}	ΔE_{MM}
I2 (M2)	0.0	0.0	0.0
$\mathbf{TS_{I2-I3}}$ (M2)	8.9	7.0	1.9
I3 (M2)	−0.1	−1.3	1.2
I2 (M3)	0.0	0.0	0.0
$\mathbf{TS_{I2-I3}}$ (M3)	9.5	7.4	2.1
I3 (M3)	2.6	1.8	0.8
I2 (M6)	0.0	0.0	0.0
$\mathbf{TS_{I2-I3}}$ (M6)	8.9	6.0	2.9
I3 (M6)	−0.9	−1.4	0.5

Many attempts to locate the concerted transition state in the protein were unsuccessful, even starting from the short Co−C bond distance (∼3.0 Å). Instead, the calculations led to the stepwise hydrogen transfer transition state $\mathbf{TS_{I2-I3}}$. Thus, we have to conclude that the transition state for the concerted pathway does not exist and converges to the stepwise pathway in the protein. The barrier for the stepwise hydrogen transfer via $\mathbf{TS_{I2-I3}}$ is computed to be 8.9 kcal/mol above **I2**, as shown in Table 3, and 18.6 kcal/mol above **R** (Table S5).[46] The activation barrier in the protein is mainly determined by ΔE_{QM} (7.0 kcal/mol), and the MM part further destabilizes $\mathbf{TS_{I2-I3}}$ by ∼1.9 kcal/mol.[47] The reaction barrier for the hydrogen transfer in the protein is considerably lower than that in the gas phase, mostly owing to the higher stability of **I2**. In addition, in the gas phase, additional hydrogen bonds between the ribose and the substrate were found in **IIS** and **IIIS**, but they are lost in $\mathbf{TS_{IIS\text{-}IIIS}}$. In protein, no such hydrogen bonds can be formed in **I2**, $\mathbf{TS_{I2-I3}}$, and **I3**, due to the confinement of the protein. In other words, MMCM perfectly positions the substrate, the Ado moiety, and the nearby residues for the Co−C bond cleavage and hydrogen transfer (substrate preorganization), which also avoids other side reactions with the reactive radical species. Therefore, the stabilization of the reactant and product complexes in the gas phase is suppressed by the protein, and in turn, the barrier is reduced in the protein. The substrate radical intermediate **I3** in the protein is essentially isoenergetic with the intermediate **I2**. The QM contribution is a little more favorable for **I3** than **I2** by 1.3 kcal/mol, but it is canceled out by the MM contribution. It is in line with the AM1/MM calculations in MMCM and the high-level DFT/MM calculations in GluMut,[10d,k] but a 10 kcal/mol thermodynamic driving force was added in the EVB calculations in MMCM.[10c] The calculated key structures for the hydrogen transfer step in the protein are displayed in Figure 5 as well as Figure S14. Very interestingly, the stepwise transition state $\mathbf{TS_{I2-I3}}$ in the protein has similar C5′···H and H···C_{sub} distances (approximately 1.37 and 1.32 Å) to those in the stepwise and concerted transition states in the gas phase (Figure S13). The computed Co···C5′ distance in $\mathbf{TS_{I2-I3}}$ is 4.41 Å, which is even longer than that in **I2** and **I3** by 0.39

(40) Two other concerted transition states ($\mathbf{TS'_{IC\text{-}IIIC}}$ and $\mathbf{TS''_{IC\text{-}IIIC}}$) with a different conformation of the ribose and different position of the substrate were also located. They are slightly higher in energy than $\mathbf{TS_{IC\text{-}IIIC}}$ (Figure S13). In the gas phase, a very small imaginary frequency of 7*i* and 5*i* cm^{-1} was found in the **Sub•/Arg** and **IIIC**, respectively.

(41) The electrostatic interaction is estimated from the energy of the whole QM system subtracting the total energy for completely separating the QM part of the corrin ring and the imidazole from the rest of the QM parts. The electrostatic interaction with the corrin ring and the imidazole is roughly−15.4 kcal/mol for $\mathbf{TS_{IC\text{-}IIIC}}$ and−6.2 kcal/mol for $\mathbf{TS_{I2\text{-}I3}}$. It should be noted that the above-mentioned electrostatic interactions are overestimated, particularly for **TSIC-IIIC**, as the isolated fragments are not relaxed.

(42) (a) Bigeleisen, J.; Mayer, M. G. *J. Chem. Phys.* **1947**, *15*, 261. (b) Melander, L.; Saunders, W. H., Jr. *Reaction Rates of Isotopic Molecules*; Wiley and Sons: New York, 1980.

(43) Anisimov, V.; Paneth, P. *J. Math. Chem.* **1999**, *26*, 75.

(44) Chowdhury, S.; Banerjee, R. *J. Am. Chem. Soc.* **2000**, *122*, 5417.

(45) Wigner, E. *Z. Phys. Chem. B* **1932**, *19*, 203.

(46) It should be mentioned that the quantum tunneling effect on the hydrogen transfer step was not considered herein (refs 1, 2, 6, and 10a).

(47) In terms of $\ddot{A}E_{QM}$, the reaction barrier and energy for the hydrogen transfer relative to **I2** in the protein are similar to those relative to the isolated intermediates **II** to **III** in the gas phase.

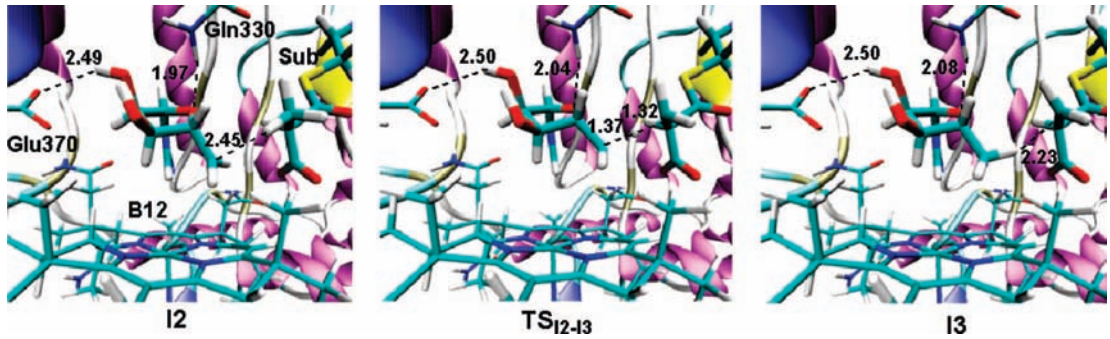

Figure 5. ONIOM-optimized structures, **I2** (left), $\mathbf{TS_{I2-I3}}$ (middle), and **I3** (right), for the hydrogen transfer in the protein for M2. Some important distances are also shown in Å.

and 0.30 Å, respectively (Table S7). It is also much longer than in $\mathbf{TS_{IC\text{-}IIIC}}$ in the gas phase. This is because in the protein the carbon radical (C5′) of the ribose has to approach the substrate to abstract the hydrogen atom in $\mathbf{TS_{I2-I3}}$. It should be noted that the Co···C5′ distance in $\mathbf{TS_{IC\text{-}IIIC}}$ and $\mathbf{TS_{I2-I3}}$ is much longer than that for the bond breaking transition state $\mathbf{TS_{I1-I2}}$ (2.68 Å) in the protein.[48]

Why is the concerted pathway unfavorable in the MMCM protein? Several factors should contribute to the difference between the gas phase and the protein. First, in the gas phase, the energy barrier for the Co−C bond cleavage is very large and the bond dissociated product **II** is highly unstable. In addition, the stepwise transition state is less favorable than the concerted transition state in the gas phase, because the interaction with the cob(II)alamin radical, the sole source of extra stabilization in the gas phase, stabilizes the concerted TS, whereas this stabilization does not exist in the stepwise TS.

In MMCM, the reaction barrier for the Co−C bond cleavage is considerably reduced and the bond cleavage state **I2** is significantly stabilized by the protein. Nevertheless, there is a quite small thermodynamic driving force to afford **I3** from **I2** in the protein (Table 3).[49] Moreover, the stepwise hydrogen transfer pathway can also be stabilized by the presence of the cob(II)alamin radical.[41] Due to the cage effect, the cob(II)alamin radical could also function as the conductor in the stepwise route via $\mathbf{TS_{I2-I3}}$, in which the spin density of Co, C5′, and C_{sub} is −0.97, +0.52, and +0.47, respectively. It should be stressed that, after the Co−C bond cleavage transition state $\mathbf{TS_{I1-I2}}$, ΔE_{QM} for the Co−C bond cleavage becomes very flat, indicating a very similar interaction between the Ado (or ribose) and the cob(II)alamin, as already seen in Figures 1, 3, and S6. The flat PES of ΔE_{QM} was also observed in GluMut.[10d] As previously discussed regarding the MM effect, the nearby residues favor **I2**. Moreover, distortion of the Ado moiety is needed for the hydrogen transfer (Table S7 and Figure S14). The shorter the C5′···Co distance in the hydrogen transfer transition state, the more distortions of the Ado moiety and the substrate are required for the hydrogen transfer process. Therefore, distortions of the Ado and the substrate, the smaller interaction with the nearby residues, as well as the small thermodynamic driving force to form the substrate radical, disfavor the proposed concerted pathway. The concerted pathway might take place if the substrate and the nearby residues could freely move closer to the carbon radical of the Ado moiety.

Since the C5′···H and C_{sub}···H distances are very similar in the concerted and stepwise transition states in the gas phase and the stepwise transition state in the protein, we examined an estimated potential energy profile for the concerted pathway by performing relaxed scan calculations at various Co...C5′ distances with fixed C5′···H and C_{sub}···H distances of $\mathbf{TS_{I2-I3}}$, as shown in Figure S15.[50] These calculations should qualitatively explain why the concerted pathway is not favorable in the protein. Although such a constrained optimization could slightly overestimate the barrier derived from the QM energy, the overall PES for the concerted route is found to be not favorable in the protein. Both the QM and MM effects disfavor the hydrogen transfer with decreasing the Co···C5′ distance. In addition, as shown in Figure S16, more distortions of the Ado moiety and the substrate were found when the Co···C5′ distance is reduced. Moreover, the Co(II) center is pushed upward, which weakens the interaction between the Co and the His610 ligand.

The QM effect of Glu370 on the stepwise and concerted pathways in the protein was investigated by M3. We could not locate the concerted transition state using this model either. The calculated activation barrier of the hydrogen transfer relative to **I2** slightly increases to 9.5 kcal/mol for M3, as shown in Table 3. Also, **I3** is calculated to be less stable than **I2** by 2.6 kcal/mol. The Co···C5′ distances in **I2** and **I3** are 3.95 and 4.12 Å for M3, respectively, similar to those for M2 (Table S7). In $\mathbf{TS_{I2-I3}}$, the Co···C5′, C5′···H, and H···C_{sub} distances are 4.42, 1.31, and 1.39 Å for M3, respectively, which are changed very little from the QM models. Likewise, the Co···C5′ bond has to be further elongated in $\mathbf{TS_{I2-I3}}$ for M3. As a whole, the Glu370 has a negligible QM effect on the hydrogen transfer process, although it effectively facilitates the Co−C bond homolytic cleavage (see section 3.2).

The final model we studied is M6 in Scheme 3, which includes the adenine moiety in the QM model part for the hydrogen transfer step. The concerted transition state again cannot be located for M6, but the stepwise hydrogen transfer transition state was located. The potential profile of the

(48) For GluMut, the calculated Co···C5′ distance in the concerted transition state is ~3.23 Å in the gas phase (ref 10b), which is similar to that for the bond dissociated state for conformation B in the crystal structure (3.17 Å) and in the QM/MM study 3.48 Å (refs 10d and 34).

(49) According to G2(MP2) calculations, the hydrogen transfer reaction from the substrate (**Sub**) to the Ado radical (**Ado•**) is slightly exothermic by 3.3 kcal/mol (without ZPC) Curtiss, L. A.; Raghavachari, K.; Pople, J. A. *J. Chem. Phys.* **1993**, *98*, 1293.

(50) The spin densities of Co, C5′, and C_{sub} for the key ONIOM-optimized structures are shown in Table S8 of the Supporting Information.

hydrogen transfer step for M6 is similar to that for M2 and M3, as shown in Table 3. For instance, a similar activation barrier relative to **I2** is obtained for models M2 and M6 (8.9 kcal/mol) but increases to 21.8 kcal/mol with respect to **R** in M6.[46] The Co···C5′, C5′···H, and H···C_{sub} distances in $\mathbf{TS_{I2-I3}}$ for M6 are also similar to those for M2 and M3 (Figures 5, S17−S18 and Table S7). **I3** is slightly more stable than the Ado radical intermediate **I2** by 0.9 kcal/mol for M6. As a whole, the QM effect of the adenine on the energetics and structures of the hydrogen transfer step is also small, since the adenine is far from the reacting substrate.

To sum up, the previously poorly understood hydrogen transfer in MMCM is studied and analyzed in detail by the current ONIOM calculations. The QM effect of Glu370 and the adenine on the energetics and geometries of the hydrogen transfer is insignificant. The effective barrier for the hydrogen transfer should be further reduced, when the quantum tunneling effect is considered. Consequently, the hydrogen transfer transition state could become similar or even lower in energy than the Co−C bond cleavage transition state (Tables 3 and S5). The concerted pathway is unfavorable in the protein in all QM models (M2, M3, and M6). Several factors were shown to facilitate the stepwise pathway in MMCM. The Co−C bond cleavage process is highly promoted by the protein. Especially, the interaction of the nearby residues with the Ado favors the bond dissociation. Moreover, the distortion of the Ado and the substrate is increased with the decrease in Co−C bond distance. Furthermore, due to the cage effect, both the stepwise and proposed concerted hydrogen transfer pathways can be stabilized by the presence of the cob(II)alamin.[51] The concerted pathway might occur, if the substrate and the nearby residues could freely approach the Ado radical for the hydrogen transfer prior to the complete Co−C bond cleavage.

The concerted mechanism of the Co−C cleavage coupled with the hydrogen transfer has recently been proposed.[2a,6b] Such a new mechanism was supported by the very recent gas-phase calculations on GluMut and the EVB simulations on MMCM.[10b,c] It should be noted that the hydrogen transfer product was calculated to be much more favorable than the Co−C bond cleavage state by more than 10 kcal/mol in these two studies,[10b,c] which therefore promotes and supports the recently proposed concerted mechanism. However, by including the interactions of the proteins and using more accurate QM/MM methods, a very small driving force for the hydrogen step was found in our study on MMCM and the previous study on GluMut.[10d] Several protein effects are also pinpointed not to favor the new concerted mechanism in this study. On the other hand, the exceptionally large measured KIE effect in MMCM was reproduced by the stepwise pathway in recent AM1/CHARMM calculations.[10a]

4. Conclusions

In the present work, the substantial protein effect on the homolytic Co−C bond cleavage followed by the less understood hydrogen transfer in the MMCM-catalyzed 1,2-rearrangement of methylmalonyl-CoA to succinyl-CoA has been investigated in detail by means of the DFT and ONIOM(DFT/AMBER) methods. Several QM models containing the residues crucial for these two key steps were adopted. The key findings are summarized as follows:

1. The Co−C bond dissociation energy in the gas phase is largely reduced, as much as ∼28 kcal/mol for the QM model M1, in the protein. Several factors are found to contribute to such a significant protein effect: the cage effect (∼5 kcal/mol), the geometric distortion of the coenzyme in the bound state **R** (mainly from the Ado, approximately 6 kcal/mol for M1 and 8 kcal/mol for M4), and the protein MM effect (approximately 17 kcal/mol for M1 and 9 kcal/mol for M4). Several residues, such as Gln330 and, particularly, Glu370,[10c] play dominant roles in stabilizing the Co−C bond cleavage state **I2**, since the dissociated Ado radical approaches these nearby residues and forms stronger hydrogen bonds. The most critical residue, Glu370, evaluated by the QM method, promotes the Co−C bond cleavage by ∼9−11 kcal/mol ($\Delta\Delta E_{ONIOM}$). These factors cooperatively facilitate the Co−C bond cleavage in the protein. Conformation of the flexible Ado in MMCM is also found to be finely tuned for the Co−C bond cleavage step.

2. A large protein effect on the hydrogen transfer step is also observed, as well as the feasibility of the newly proposed concerted mechanism is examined. The Co−C bond cleavage and the hydrogen transfer occur in a stepwise manner in the protein, while the concerted pathway is more favorable by ∼8 kcal/mol in the gas phase. Due to the cage effect, both stepwise and concerted pathways can be stabilized by the cob(II)alamin in the protein. The Ado moiety loses some interaction with the nearby residues, when shortening the Co−C bond (i.e., the protein MM effect). Moreover, the Ado and the substrate are more distorted in the assumed concerted transition state. The reaction barrier for the hydrogen transfer is also significantly reduced from 47 kcal/mol in the gas phase to ∼19 kcal/mol, due to the very high stability of the bond cleavage state **I2** and the substrate preorganization. The QM effect of Glu370 and the adenine group on the hydrogen transfer is very small. We do not rule out the new concerted mechanism in the B_{12}-dependent enzyme systems,[2a,6b] when the protein and substrate are flexible or/and the hydrogen transfer process is endowed with a significant driving force.

Investigations of the origin of the large catalytic effect on the Co−C bond cleavage and the hydrogen transfer in MMCM are very challenging. The QM part of the coenzyme has to be very large and treated by a more accurate QM method to adequately describe the energetics and geometry of the very strained bound state and the very strong hydrogen bond, although the strain energy of the coenzyme was suggested to be overestimated by the energy minimization approach,[10c] presumably due to the lack of the protein sampling. It should be noted that the activation of AdoCbl was experimentally shown to be predominantly determined by the enthalpic factor (91%) in the enzymes, rather than the entropic factor.[2a] Our extensive QM and ONIOM calculations delineate the main energetic and structural features of the first two important steps in MMCM. The conclusive origin of the large protein effect in MMCM would be verified by very demanding and accurate QM/MM calculations in the free energy surface, which is currently in progress in our laboratory.

(51) As shown in Figure S13, the concerted transition state $\mathbf{TS''_{IC\text{-}IIC}}$ with the shortest Co···C bond (3.57 Å) was calculated to be the least favorable concerted transition state. Therefore, in addition to the stabilization by the presence of the cob(II)alamin, the energetics of the transition state was shown to be also influenced by other factors (such as hydrogen bonding and conformation of the ribose).

Acknowledgment. We thank Drs. Thom Vreven, Marcus Lundberg, Ahmet Altun, and Renata A. Kwiecien for useful discussions and suggestions. We also thank Prof. Helder M. Marques for giving AMBER parameters for the B_{12} cofactor. This work is in part supported by the Japan Science and Technology Agency (JST) with a Core Research for Evolutional Science and Technology (CREST) grant in the Area of High Performance Computing for Multiscale and Multiphysics Phenomena. The computational resource at the Research Center of Computer Science (RCCS) at the Institute for Molecular Science (IMS) is also acknowledged.

Supporting Information Available: Complete citation of refs 19 and 21, Figures S1−S18, Tables S1−S8, Cartesian coordinates and absolute energies in the gas phase. This material is available free of charge via the Internet at http://pubs.acs.org.

JA807677Z